# Linear relationship between temperature and the apparent reaction rate constant of hydroxyl radical with 4-chlorobenzoic acid

Kohei Kawaguchi [a]*, Taira Hidaka [a], and Fumitake Nishimura [a]

[a]*Graduate School of Engineering, Kyoto University, Kyoto, Japan*

**kawaguchi.kohei.24v@st.kyoto-u.ac.jp*

# Linear relationship between temperature and the apparent reaction rate constant of hydroxyl radical with 4-chlorobenzoic acid


## ABSRACT

4-Chlorobenzoic acid (*p*-CBA) is frequently used as a hydroxyl radical (HO·) probe substance in studies of ozonation and advanced oxidation processes. However, the temperature dependence of the reaction between HO· and *p*-CBA remains unclear. In this context, we identified the relationship between temperature ($T$, K) and the apparent second-order reaction rate constant of HO· with *p*-CBA ($k_{\mathrm{HO}\cdot,p\text{-CBA}}(T)$, $\mathrm{M^{-1}\ s^{-1}}$): $k_{\mathrm{HO}\cdot,p\text{-CBA}}(T) = 8.2 \times 10^7\ T - 1.96 \times 10^{10}$. They were measured by a novel competitive method using 2-methylpropan-2-ol (tert-butyl alcohol) as a reference substance in the range of 1.0–40.0°C. The linear regression equation was more appropriate than the exponential regression equation to express this relationship. More generally, our simulation shows that the linear regression equation can be more accurate than the exponential regression equation to express the relationship between temperature and apparent reaction rate constants of HO·.



KEYWORDS: ozone, advanced oxidation process, 2-methylpropan-2-ol, competitive method, Arrhenius equation, Rct value


## Introduction

Hydroxyl radical (HO·) plays a crucial role in removing contaminants in ozonation and advanced oxidation processes as it reacts very rapidly with most substances (Buxton et al., 1988; Peter and Von Gunten, 2007). Hence, it is vital to know the concentration of HO· in these processes, although direct HO· quantification is almost impossible. Therefore, probe substances that react with HO· and barely react with other oxidizing agents are used for indirect HO· quantification.

4-Chlorobenzoic acid (*p*-CBA) is widely used as a probe substance (Elovitz and von Gunten, 1999). The reaction rate constant of HO· with *p*-CBA is reported as $4.5 \times 10^9$ $\mathrm{M^{-1}\ s^{-1}}$ (Zona et al., 2010) and $5.0 \times 10^9$ $\mathrm{M^{-1}\ s^{-1}}$ (Neta and Dorfman, 1968) at room temperature. However, papers reporting the relationship between temperature and the reaction rate constant of HO· with *p*-CBA were not found. In contrast to HO·, the reaction rate constant of *p*-CBA with ozone is small (< 0.15 $\mathrm{M^{-1}\ s^{-1}}$) (Yao and Haag, 1991). Therefore, it can be interpreted that *p*-CBA does not react with ozone but only with HO· during ozonation and advanced oxidation processes (Elovitz and von Gunten, 1999).

Since water treatment is usually carried out in the range of 0–40°C, experiments using *p*-CBA can be performed at temperatures of the same range. At that time, using reaction rate constants measured at room temperature results in errors during the analysis of results.

For example, in the field of ozonation, the $R_{\mathrm{ct}}$ value defined by Eq. (1), is widely used (Elovitz and

von Gunten, 1999).

$$R_{ct} \equiv \frac{\int [HO\cdot]dt}{\int [O_3]\,dt} \quad (1)$$

Where, $[HO\cdot]$ and $[O_3]$ are the concentrations of HO· and ozone (M), respectively. Except in the early stages of the reaction, $R_{ct}$ is reported to be constant (Buffle et al., 2006). Thus, $R_{ct}$ can be used to estimate HO· concentration from ozone concentration. By adding *p*-CBA to the sample water in advance, $\int [HO\cdot]dt$ in Eq. (1) can be calculated from Eq. (2) (Elovitz and von Gunten, 1999):

$$\int [HO\cdot]dt = \frac{1}{k_{HO\cdot,p\text{-CBA}}} \ln \frac{[p\text{-CBA}]_0}{[p\text{-CBA}]} \quad (2)$$

Where, $k_{HO\cdot,p\text{-CBA}}$ is the apparent reaction rate constant of HO· with *p*-CBA ($M^{-1}\ s^{-1}$), and $[p\text{-CBA}]_0$ is the initial concentration of *p*-CBA (M). $\int [O_3]\,dt$ in Eq. (1) is calculated by measuring the change in ozone concentration over time during the reaction. $R_{ct}$ is reported to increase with increasing temperature (Elovitz et al., 2000). However, for the analysis, the same $k_{HO\cdot,p\text{-CBA}}$ was used even at different temperatures resulting in the effect of temperature on $R_{ct}$ to be overestimated. Therefore, to reveal the temperature dependence of $k_{HO\cdot,p\text{-CBA}}$ would lead to a more accurate understanding of the HO· concentration in ozone treatment.

The most optimal way to study HO· reactions is to directly measure the decrease of reactants using pulse radiolysis (Buxton et al., 1988). However, this device is expensive and not readily available to many water treatment researchers. To solve this issue, we develop a new competitive method that can be used to measure the temperature dependence of the reaction rate constants of HO·.

Apparent reaction rate constant of the bimolecular reaction can be written as Eq. (3):

$$k_{app} = \frac{k_{che}\, k_{dif}}{k_{che} + k_{dif}} \quad (3)$$

Where, $k_{app}$ is the apparent reaction rate constant ($M^{-1}\ s^{-1}$), $k_{che}$ is the chemical reaction rate constant ($M^{-1}\ s^{-1}$), and $k_{dif}$ is the diffusion-limited rate constant ($M^{-1}\ s^{-1}$). $k_{che}$ can be written as Eq. (4) using the Arrhenius equation:

$$k_{che} = A \exp\left(-\frac{E}{RT}\right) \quad (4)$$

Where, $A$ is the pre-exponential factor ($M^{-1}\ s^{-1}$), $E$ is the activation energy (kJ $mol^{-1}$), $R$ is the gas constant (kJ $mol^{-1}\ K^{-1}$), and $T$ is the temperature (K). $A$, $E$, and $R$ are usually temperature-independent constants. $k_{dif}$ can be written as Eq. (5) using the Smoluchowski equation (Elliot et al., 1990):

$$k_{\mathrm{dif}} = 4 \times 10^3 \pi N_0 D r \tag{5}$$

Where, $N_0$ is the Avogadro constant ($\mathrm{mol}^{-1}$), $D$ is the sum of the diffusion coefficients in water of two molecules ($\mathrm{m^2\ s^{-1}}$), $r$ is the reaction radius (m). $N_0$ and $r$ are usually temperature-independent constants, and $D$ is temperature-dependent. The temperature dependence of $D$ is often approximated using the Stokes-Einstein relation written as Eq. (6) (Elliot et al., 1990):

$$D = \frac{T}{T_{\mathrm{ref}}} \frac{\mu_{\mathrm{ref}}}{\mu} D_{\mathrm{ref}} \tag{6}$$

Where, $\mu$ is the viscosity of water (Pa s), and $\mu_{\mathrm{ref}}$ and $D_{\mathrm{ref}}$ are the viscosity of water and diffusion coefficient, respectively, at $T_{\mathrm{ref}}$. From Eq. (5) and (6), Eq. (7) can be derived as follows:

$$k_{\mathrm{dif}} = 4 \times 10^3 \pi N_0 \frac{T}{T_{\mathrm{ref}}} \frac{\mu_{\mathrm{ref}}}{\mu} D_{\mathrm{ref}}\, r \tag{7}$$

$\mu$ is also temperature-dependent, and the temperature dependence of it is approximated by Eq. (8) (Huber et al., 2009):

$$\mu = 280.68 \left(\frac{T}{300}\right)^{-1.9} + 511.45 \left(\frac{T}{300}\right)^{-7.7} + 61.131 \left(\frac{T}{300}\right)^{-19.6} + 0.45903 \left(\frac{T}{300}\right)^{-40.0} \tag{8}$$

In many earlier studies, the temperature dependence of the apparent reaction rate constant was described by the exponential regression equation (ERE) equivalent to the Arrhenius equation (Buxton et al., 1988). However, when Eq. (3), (4), (7), and (8) are considered together, it is not evident that the Arrhenius equation holds true for the apparent reaction rate constants.

The $T$-$k_{\mathrm{app}}$ graphs can be upward or downward convex, depending on the combination of parameters ($A$, $E$, $D_{\mathrm{ref}}$, and $r$). However, when the temperature is limited to the range of 0–40°C and considering that the activation energy of HO· is small (almost less than 20 kJ (Buxton et al., 1988)), the $T$-$k_{\mathrm{app}}$ graphs become almost straight lines. Therefore, a simulation was conducted to compare the ERE and the linear regression equation (LRE) to represent the temperature dependence of the apparent reaction rate constants of HO· in water.

This study revealed the relationship between temperature and the apparent reaction rate constant of HO· with *p*-CBA, following which the ERE of this relationship was compared with its LRE to determine the equation that more accurately describes the relationship. In addition, the accuracy of the ERE was compared with that of the LRE through simulation as the expression of relationships between temperature and apparent reaction rate constants of HO· with substances other than *p*-CBA in water. The temperature dependence of reaction rate constants of HO· with substances related to water treatment have recently received much attention (Gleason et al., 2017; McKay et al., 2011). However, in these studies, the regression equation for the temperature dependence has not been examined in detail. Therefore, the simulation results in the present study can contribute to future research on the temperature dependence of HO· reactions.

## Methods

### *Experimental Method Development*

Development overview of our novel competitive method to measure the temperature dependence of reaction rate constants of HO· is described here. HO· was generated by the reaction of ozone and hydrogen peroxide (Fischbacher et al., 2013). 2-methylpropan-2-ol (*t*-BuOH) was chosen as a reference substance because its reaction rate constants are suitable ;the apparent reaction rate constant of *t*-BuOH for ozone is small, $1.1 \times 10^{-3}$ $M^{-1}$ $s^{-1}$ (Hoigné and Bader, 1983), and for HO· is large, $6.0 \times 10^{8}$ $M^{-1}$ $s^{-1}$ (Buxton et al., 1988). Thus, the reaction of ozone with *t*-BuOH can be ignored. The details of the reaction of HO· with *t*-BuOH are described by (Flyunt et al., 2003). In addition, the diffusion-limited rate constant of the reaction between HO· and *t*-BuOH is $2.8 \times 10^{10}$ $M^{-1}$ $s^{-1}$ (Elliot et al., 1990). Therefore, from Eq. (3), since the diffusion-limited rate constant is sufficiently larger than the chemical reaction rate constant, the temperature dependence of the apparent reaction rate constant follows the chemical reaction rate constant. The apparent activation energy of the reaction is consistent at 10 kJ (Elliot and Simsons, 1984; Ervens et al., 2003); hence, it can be deemed reliable. Since our method can be implemented by almost any researcher, it can facilitate the study of the temperature dependence of HO· reactions.

### *Materials*

*p*-CBA, *t*-BuOH, hydrogen peroxide, sodium dihydrogen phosphate, disodium hydrogen phosphate dodecahydrate, and phosphoric acid of the highest purity grade were acquired from FUJIFILM Wako Pure Chemical, Japan. Indigotrisulfonic acid potassium salt was acquired from Tokyo Chemical, Japan. All stock solutions were prepared in ultrapure water (≥ 18.2MΩ).

### *Experimental Method*

An aqueous solution consisting of 0.70 μM *p*-CBA, 88 μM *t*-BuOH, and 1.0 mM phosphate buffer of pH 7.0 was used for the experiment. During the experiment, the pH values were maintained from 6.9 to 7.1. The product of the reaction between HO· and *p*-CBA might react with *t*-BuOH. Therefore, by reducing the *p*-CBA concentration so much compared to the *t*-BuOH concentration, the effect of the reaction products of HO· and *p*-CBA reacting with *t*-BuOH was made negligible. The solution (50 mL) was placed in an Erlenmeyer flask and kept at a predetermined temperature in a water bath. Temperature conditions were set to 1.0, 10.0, 20.0, 30.0, and 40.0°C. Immediately after adding 0.1 mL of 30 μM hydrogen peroxide to the solution, ozone gas with a flow rate of 70 mL $min^{-1}$ was blown into it for 10 s by a diffuser. The ozone gas concentration was 0.4 mM measured by UV OZONE MONITOR model-600 (Ebara Jitsugyo, Japan). From the time of hydrogen peroxide injection to one minute after the completion of ozone injection, the solution was stirred vigorously with a magnetic stirrer rotated at $1.8 \times 10^{3}$ rpm. Twenty minutes post the ozone gas

injection, the concentrations of *p*-CBA and *t*-BuOH were measured after confirming the absence of dissolved ozone concentration by the indigo method (Bader and Hoigné, 1981). The initial concentrations of *p*-CBA and *t*-BuOH were determined from the blanks retained under the same temperature conditions. This experiment was repeated more than three times for one temperature condition.

As the reaction system is considered to be in a complete mixed state, the change in concentration of *p*-CBA and *t*-BuOH is expressed as Eq. (9) and (10), and subsequent Eq. (11) is derived as:

$$\frac{\mathrm{d}[p\text{-CBA}]}{\mathrm{dt}} = -k_{\mathrm{HO}\cdot,p\text{-CBA}}(T)[p\text{-CBA}][\mathrm{HO}\cdot] \tag{9}$$

$$\frac{\mathrm{d}[t\text{-BuOH}]}{\mathrm{dt}} = -k_{\mathrm{HO}\cdot,t\text{-BuOH}}(T)[t\text{-BuOH}][\mathrm{HO}\cdot] \tag{10}$$

$$k_{\mathrm{HO}\cdot,p\text{-CBA}}(T) = \frac{\ln\frac{[p\text{-CBA}]_\infty}{[p\text{-CBA}]_0}}{\ln\frac{[t\text{-BuOH}]_\infty}{[t\text{-BuOH}]_0}}\, k_{\mathrm{HO}\cdot,t\text{-BuOH}}(T) \tag{11}$$

Where, the subscripts "0" and "∞" represent the concentrations before and after the reaction, respectively. $k_{\mathrm{HO}\cdot,p\text{-CBA}}(T)$ and $k_{\mathrm{HO}\cdot,t\text{-BuOH}}(T)$ are the apparent reaction rate constants for *p*-CBA and *t*-BuOH with HO· at *T*, respectively. $k_{\mathrm{HO}\cdot,t\text{-BuOH}}(T)$ is represented by Eq. (12) (Elliot and Simsons, 1984; Ervens et al., 2003):

$$k_{\mathrm{HO}\cdot,t\text{-BuOH}}(T) = 3.40 \times 10^{10} \exp\left(-\frac{10000}{RT}\right) \tag{12}$$

According to Eq. (11) and (12), the reaction rate constant of HO· with *p*-CBA was calculated at each temperature. In principle, the amount of HO· produced does not affect the calculation of $k_{\mathrm{HO}\cdot,p\text{-CBA}}(T)$. Hence, it is not affected by the ozone concentration and flow rate. From five sets of reaction rate constant and temperature, the ERE and LRE were obtained, and finally, the root-mean-squared error (RMSE) was calculated to compare the two regression equations. The RMSE is defined by the following expression:

$$\mathrm{RMSE} = \sqrt{\frac{1}{\mathrm{N}}\sum_{\mathrm{i}=1}^{\mathrm{N}}(\hat{\mathrm{y}}_\mathrm{i} - \mathrm{y}_\mathrm{i})^2} \tag{13}$$

Where, $\mathrm{N}$ is the number of data, $\hat{\mathrm{y}}_\mathrm{i}$ is the true value (experimental value), and $\mathrm{y}_\mathrm{i}$ is the regression value.

In all experiments, the maximum removal rates of *p*-CBA and *t*-BuOH were 92% and 30%, and the minimums were 54% and 14%, respectively. As the three variables $A$, $E$, and $r$ in Eq. (4) or (7) are unknown, the chemical reaction rate constant and diffusion-limited rate constant for HO· and *p*-CBA could not be calculated from the experimental data.

***Chemical analysis***

The concentration of *p*-CBA was measured by HPLC/UV (LC-10A series, Shimadzu), and the analytical conditions are listed in Table 1. The concentration of *t*-BuOH was measured by GC/MS (6890N Network GC

system and 5973 Network Mass Selective Detector, Agilent Technologies), and the analytical conditions are as shown in Table 2.

The measurements of *p*-CBA and *t*-BuOH were repeated three times for each sample, and the average value was taken as the measured value. The mean values of the relative standard deviations for each measurement of *p*-CBA and *t*-BuOH were 0.9% and 2.9%, respectively, and the standard deviations of them were 0.8% and 2.1%, respectively.

### *Simulation Method*

The objective of this simulation is to compare the accuracy of the ERE and LRE as the expression for the relationship between temperature and the apparent reaction rate constants of HO· with substances in water. After obtaining the four parameters $k_{\mathrm{che}}$, $E$, $D$, and $r$ in Eq. (4) or (7), the apparent reaction rate constant for each water temperature can be calculated. However, we were not able to find sufficient information about the distribution of these parameters. Therefore, based on each parameter's reported values, a range of possible values for each parameter was estimated. The range of $k_{\mathrm{che}}$ was set from $5 \times 10^8$ to $5 \times 10^{10}$ $M^{-1}$ $s^{-1}$ (Buxton et al., 1988). The range of $E$ was set from 0 to 20 kJ (Buxton et al., 1988). Taking into account the diffusion coefficient of HO· in water that is reported to be $2.8 \times 10^{-9}$ $m^2$ $s^{-1}$ (Codorniu-Hernández and Kusalik, 2012; Schwarz, 1969), the range of $D$ was set from $2.9 \times 10^{-9}$ to $4.8 \times 10^{-9}$ $m^2$ $s^{-1}$ (Elliot et al., 1990). The range of $r$ was set from $2 \times 10^{-10}$ to $10^{-9}$ $m^2$ $s^{-1}$(Elliot et al., 1990). Within these ranges, one million values were generated and paired for each parameter at random. Using the generated values and Eq. (3), (4), (7), and (8), the apparent reaction rate constants at 1, 10, 20, 30, and 40°C were calculated. From these values, the ERE, LRE, and RMSE of each regression were calculated, and the apparent activation energy was obtained from the ERE. Thus, the accuracy of the ERE and LRE for the relationship between temperature and apparent reaction rate constants of HO· is compared for most of the cases.

## Results and Discussion

### *Experiment*

Figure 1 shows the relationship between temperature ($T$, K) and the apparent reaction rate constant of HO· and *p*-CBA ($k_{\mathrm{HO}\cdot,p\text{-CBA}}(T)$, $M^{-1}$ $s^{-1}$). The ERE expression for it is shown below:

$$k_{\mathrm{HO}\cdot,p\text{-CBA}}(T) = 7.31 \times 10^{11} \exp\left(\frac{-12450}{RT}\right) \tag{14}$$

The error of the pre-exponential factor in Eq. (12) multiplicatively affects the pre-exponential factor in Eq. (14). For example, if the true value of the pre-exponential factor in Eq. (12) is twice the current value, then the pre-exponential factor in Eq. (14) will be doubled to $14.6 \times 10^{11}$. The error in the apparent activation

energy in Eq. (12) additively affects the apparent activation energy in Eq. (14). For example, if the true value of the apparent activation energy in Eq. (12) is 2 kJ greater than the current value, the apparent activation energy in Eq. (14) is added by 2 kJ to obtain 14.45 kJ.

The LRE expression for the relationship between temperature ($T$, K) and the apparent reaction rate constant of HO· and *p*-CBA ($k_{\mathrm{HO}\cdot,p\text{-CBA}}(T)$, $M^{-1}$ $s^{-1}$) is shown below:

$$k_{\mathrm{HO}\cdot,p\text{-CBA}}(T) = 8.2 \times 10^7 T - 1.96 \times 10^{10} \quad (15)$$

If the reaction rate at 25°C is $6.0 \times 10^8$ $M^{-1}$ $s^{-1}$ and there is an error in the apparent activation energy in Eq. (12), then $6 \times 10^6$ is added to the slope of the regression equation, and the intercept is subtracted by $1.2 \times 10^8$ per 1 kJ error of the apparent activation energy.

The RMSE of the LRE ($5.0 \times 10^7$) was smaller than that of the ERE ($1.4 \times 10^8$). Therefore, the LRE was a better regression equation than the ERE. The difference between the LRE and ERE was more significant at lower temperatures. At 1°C, based on the experimental value, the error of the LRE was −0.2% and one of the ERE was +8%.

The reaction rate at 25°C determined by the LRE, was $4.8 \times 10^9$ $M^{-1}$ $s^{-1}$, and it is close to the value reported earlier, $4.5 \times 10^9$ $M^{-1}$ $s^{-1}$ (Zona et al., 2010) and $5.0 \times 10^9$ $M^{-1}$ $s^{-1}$ (Neta and Dorfman, 1968). This justified the experimental methods in this study.

Based on the LRE, a ratio of the reaction rate constant at each temperature to one at 25°C is 0.59 at 1°C, 0.74 at 10°C, 0.92 at 20°C, 1.1 at 30°C, and 1.3 at 40°C. If the temperature dependence of the reaction rate constant is not taken into account when estimating the concentration of HO· using *p*-CBA, the HO· concentration will be overestimated by this much.

The temperature dependence of $R_{\mathrm{ct}}$ has been evaluated in previous studies (Elovitz et al., 2000). It was $6.0 \times 10^{-9}$ $M^{-1}$ $s^{-1}$ at 5°C, $1.5 \times 10^{-8}$ $M^{-1}$ $s^{-1}$ at 15°C, $3.1 \times 10^{-8}$ $M^{-1}$ $s^{-1}$ at 25°C, and $8.5 \times 10^{-8}$ $M^{-1}$ $s^{-1}$ at 35°C. In this study, the same rate constants of HO· with *p*-CBA were used for different temperatures. To account for temperature dependence, $R_{\mathrm{ct}}$ is modified to $9.1 \times 10^{-9}$ $M^{-1}$ $s^{-1}$ at 5°C, $1.8 \times 10^{-8}$ $M^{-1}$ $s^{-1}$ at 15°C, $3.1 \times 10^{-8}$ $M^{-1}$ $s^{-1}$ at 25°C, and $7.3 \times 10^{-8}$ $M^{-1}$ $s^{-1}$ at 35°C. The temperature dependence of $R_{\mathrm{ct}}$ becomes smaller than what has been reported. A full-scale ozone treatment has been simulated using $R_{\mathrm{ct}}$ to estimate the HO· concentration (Kaiser et al., 2013; Zimmermann et al., 2011). Therefore, the results of this experiment can be applied to control of ozonation treatment where the temperature fluctuates with the season.

***Simulation***

The relationship between the apparent activation energy and the RMSE of the ERE and LRE is shown in Figure 2, and their difference is shown in Figure 3. Since the distribution of the simulation parameters is random, Figure 3 is not very quantitative. Nevertheless, it shows that the LRE is almost always more accurate than the ERE in the range where the apparent activation energy is below 10 kJ. Therefore, in this case, the temperature dependence of HO· reaction should be reported with the LRE using data excluding too high

temperature data. Even when the apparent activation energy is between 10 and 18 kJ, the LRE can be accurate than the ERE. In this case, it is reasonable to calculate both the LRE and ERE and use the regression equation with less error. When the apparent activation energy is above 18 kJ, the ERE is accurate than the LRE.

From Eq. (16), the error in the reaction rate constant also affects the estimation of the residual rate of substances removed by HO·. It is difficult to state in general how much difference occurs between the LRE and ERE because it strongly depends on the experimental error. However, in this study, the fact that the difference was as much as 8% for the reaction of HO· and *p*-CBA at 1°C in this study emphasizes the significance of comparing the regression equations.

**Conclusions**

The relationship between temperature ($T$, K) and the apparent second-order reaction rate constant of HO· and *p*-CBA ($k_{\mathrm{HO}\cdot,p\text{-CBA}}(T)$ ($\mathrm{M^{-1}\ s^{-1}}$) in the range of 1.0–40.0°C has been revealed, given as $k_{\mathrm{HO}\cdot,p\text{-CBA}}(T) = 8.2 \times 10^7 T - 1.96 \times 10^{10}$. They were measured by a novel competitive method using *t*-BuOH, and the measured reaction rate is in good agreement with the earlier published values. Our method is convenient because it does not require any special equipment.

Furthermore, the LRE is showed to be almost always more accurate than the ERE in representing the temperature dependence of HO· reaction in water when the temperature range is 1.0–40.0°C and when the apparent activation energy of the reaction is less than 10 kJ. Even when the apparent activation energy is between 10 and 18 kJ, the LRE can be accurate than the ERE. Moreover, in this study of HO· and *p*-CBA reaction, the LRE showed less error than the ERE.

# Reference


1. Bader, H., and Hoigné, J. (1981). Determination of ozone in water by the indigo method. Water Res. *15*, 449–456.
2. Buffle, M.-O., Schumacher, J., Salhi, E., Jekel, M., and von Gunten, U. (2006). Measurement of the initial phase of ozone decomposition in water and wastewater by means of a continuous quench-flow system: application to disinfection and pharmaceutical oxidation. Water Res. *40*, 1884–1894.
3. Buxton, G.V., Greenstock, C.L., Helman, W.P., and Ross, A.B. (1988). Critical Review of rate constants for reactions of hydrated electrons, hydrogen atoms and hydroxyl radicals (·OH/·O− in Aqueous Solution. J. Phys. Chem. Ref. Data *17*, 513–886.
4. Codorniu-Hernández, E., and Kusalik, P.G. (2012). Mobility mechanism of hydroxyl radicals in aqueous solution via hydrogen transfer. J. Am. Chem. Soc. *134*, 532–538.
5. Elliot, A.J., and Simsons, A.S. (1984). Rate constants for reactions of hydroxyl radicals as a function of temperature. Radiat. Phys. Chem. *24*, 229–231.
6. Elliot, J.A., McCracken, D.R., Buxton, G.V., and Wood, N.D. (1990). Estimation of rate constants for near-diffusion-controlled reactions in water at high temperatures. J. Chem.

Soc. Faraday Trans. *86*, 1539–1547.

7. Elovitz, M.S., and von Gunten, U. (1999). Hydroxyl Radical/Ozone Ratios During Ozonation Processes. I. The Rct Concept. Ozone: Sci. Eng. *21*, 239–260.
8. Elovitz, M.S., von Gunten, U., and Kaiser, H.-P. (2000). Hydroxyl Radical/Ozone Ratios During Ozonation Processes. II. The Effect of Temperature, pH, Alkalinity, and DOM Properties. Ozone: Sci. Eng. *22*, 123–150.
9. Ervens, B., Gligorovski, S., and Herrmann, H. (2003). Temperature-dependent rate constants for hydroxyl radical reactions with organic compounds in aqueous solutions. Phys. Chem. Chem. Phys. *5*, 1811–1824.
10. Fischbacher, A., von Sonntag, J., von Sonntag, C., and Schmidt, T.C. (2013). The (•)OH radical yield in the $H_2O_2 + O_3$ (peroxone) reaction. Environ. Sci. Technol. *47*, 9959–9964.
11. Fischbacher, A., Löppenberg, K., von Sonntag, C., and Schmidt, T.C. (2015). A New Reaction Pathway for Bromite to Bromate in the Ozonation of Bromide. Environ. Sci. Technol. *49*, 11714–11720.
12. Flyunt, R., Leitzke, A., Mark, G., Mvula, E., Reisz, E., Schick, R., and von Sonntag, C. (2003). Determination of •OH, $O_2$•-, and Hydroperoxide Yields in Ozone Reactions in Aqueous Solution. J. Phys. Chem. B *107*, 7242–7253.
13. Gleason, J.M., McKay, G., Ishida, K.P., and Mezyk, S.P. (2017). Temperature dependence of hydroxyl radical reactions with chloramine species in aqueous solution. Chemosphere *187*, 123–129.
14. Hoigné, J., and Bader, H. (1983). Rate constants of reactions of ozone with organic and inorganic compounds in water—I: Non-dissociating organic compounds. Water Res. *17*, 173–183.
15. Huber, M.L., Perkins, R.A., Laesecke, A., Friend, D.G., Sengers, J.V., Assael, M.J., Metaxa, I.N., Vogel, E., Mareš, R., and Miyagawa, K. (2009). New International Formulation for the Viscosity of $H_2O$. J. Phys. Chem. Ref. Data *38*, 101–125.
16. Kaiser, H.-P., Köster, O., Gresch, M., Périsset, P.M.J., Jäggi, P., Salhi, E., and von Gunten, U. (2013). Process Control For Ozonation Systems: A Novel Real-Time Approach. Ozone: Sci. Eng. *35*, 168–185.
17. McKay, G., Dong, M.M., Kleinman, J.L., Mezyk, S.P., and Rosario-Ortiz, F.L. (2011). Temperature dependence of the reaction between the hydroxyl radical and organic matter. Environ. Sci. Technol. *45*, 6932–6937.
18. Neta, P., and Dorfman, L.M. (1968). Pulse Radiolysis Studies. XIII. Rate Constants for the Reaction of Hydroxyl Radicals with Aromatic Compounds in Aqueous Solutions. In Radiation Chemistry, (AMERICAN CHEMICAL SOCIETY), 222–230.
19. Peter, A., and Von Gunten, U. (2007). Oxidation kinetics of selected taste and odor compounds during ozonation of drinking water. Environ. Sci. Technol. *41*, 626–631.
20. Schwarz, H.A. (1969). Applications of the spur diffusion model to the radiation

chemistry of aqueous solutions. J. Phys. Chem. *73*, 1928–1937.

21. Tang, G., Adu-Sarkodie, K., Kim, D., Kim, J.-H., Teefy, S., Shukairy, H.M., and Mariñas, B.J. (2005). Modeling Cryptosporidium parvum oocyst inactivation and bromate formation in a full-scale ozone contactor. Environ. Sci. Technol. *39*, 9343–9350.
22. Yao, C.C.D., and Haag, W.R. (1991). RATE CONSTANTS FOR DIRECT REACTIONS OF OZONE WITH SEVERAL DRINKING WATER CONTAMINANTS. Plan. Perspect. *761*, 773.
23. Zimmermann, S.G., Wittenwiler, M., Hollender, J., Krauss, M., Ort, C., Siegrist, H., and von Gunten, U. (2011). Kinetic assessment and modeling of an ozonation step for full-scale municipal wastewater treatment: micropollutant oxidation, by-product formation and disinfection. Water Res. *45*, 605–617.
24. Zona, R., Solar, S., Getoff, N., Sehested, K., and Holcman, J. (2010). Reactivity of OH radicals with chlorobenzoic acids—A pulse radiolysis and steady-state radiolysis study. Radiat. Phys. Chem. *79*, 626–636.

**Table1** Analytical conditions of HPLC/UV for the measurement of *p*-CBA

| Parameters | Conditions |
|---|---|
| Column | Inert Sustain C18 HP 3 μm: i.d. 4.6 mm × 20 mm<br>Inert Sustain C18 HP 3 μm: i.d. 4.6 mm × 150 mm<br>GL Sciences, Japan |
| Eluent, Flow rate | Methanol, 0.52 mL $min^{-1}$<br>1% aqueous phosphoric acid, 0.28 mL $min^{-1}$ |
| Oven temperature | 30°C |
| Injection volume | 100 μL |
| Detection wavelength | 234 nm (Retention time: 7.9 min) |

**Table2** Analytical conditions of GC/MS for the measurement of *t*-BuOH

| Parameters | Conditions | | |
|---|---|---|---|
| Column | DB-WAX Ultra Inert:<br>30 m × i.d. 0.25 mm × film thickness 0.5 μm<br>Agilent Technologies, USA | | |
| Carrier gas | He at 1.5 mL $min^{-1}$ | | |
| Injection volume | 0.4 μL (injection mode: split 50:1) | | |
| Oven temperature | 40°C (3.5 min) to 150°C (3 min) at 40°C $min^{-1}$ | | |
| Injector temperature | 230°C | Transfer temperature | 230°C |
| Ion source temperature | 230°C | Quadrupole temperature | 150°C |
| m/z of selected ion | 59 (Retention time: 2.7 min) | | |

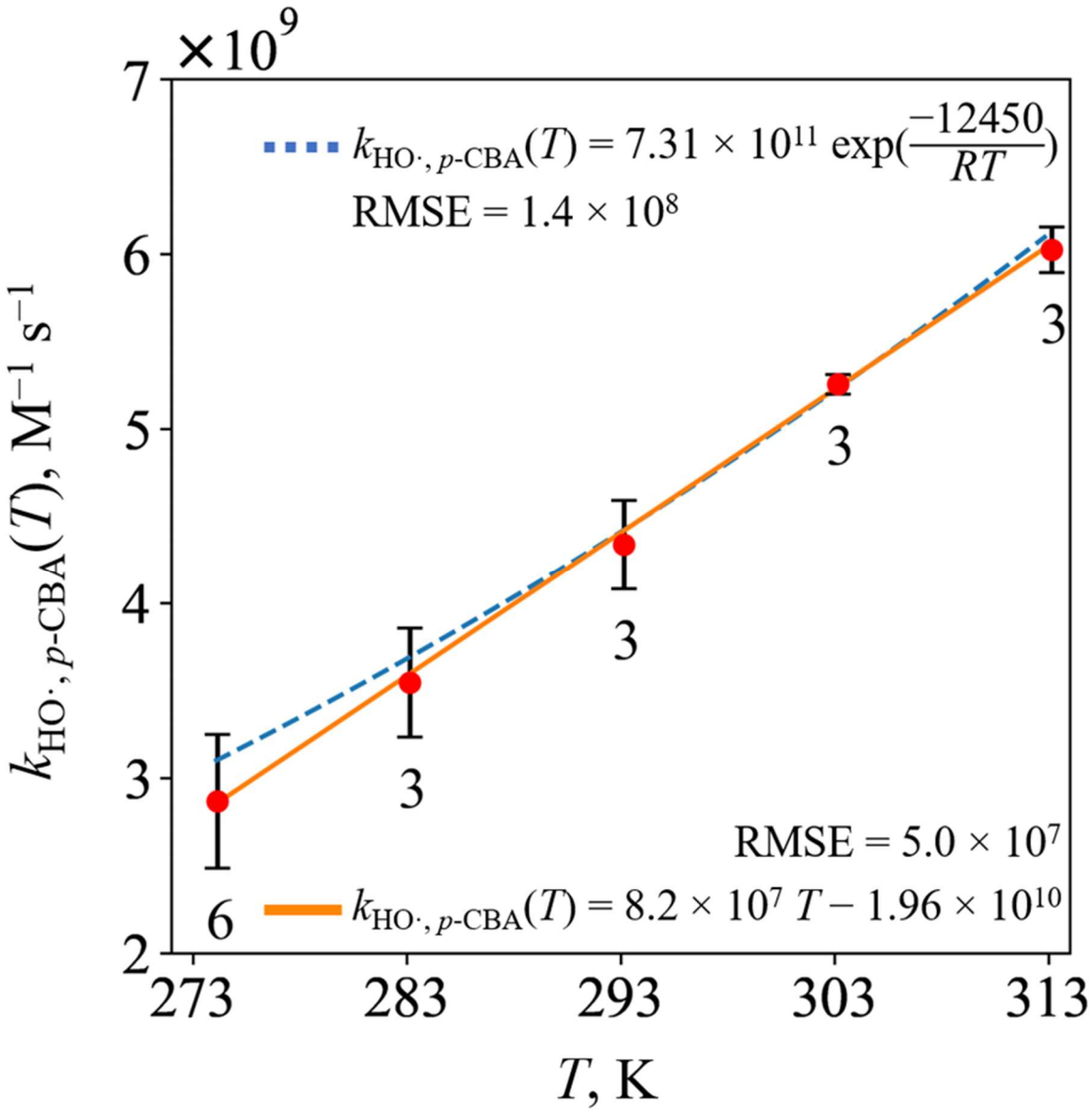


**Figure 1** Relationship between temperature ($T$, K) and the apparent reaction rate constant of HO· and *p*-CBA ($k_{HO\cdot,p\text{-CBA}}(T)$, $M^{-1}$ $s^{-1}$). The ERE is represented by the dotted line and the LRE is represented by the solid line. The error bars indicate 95% confidence interval when there is no error in Eq. (12). The numbers below error bars represent the number of repeated measurements. The ERE and LRE is calculated with weights on the inverse of the square of the confidence interval of each plot.

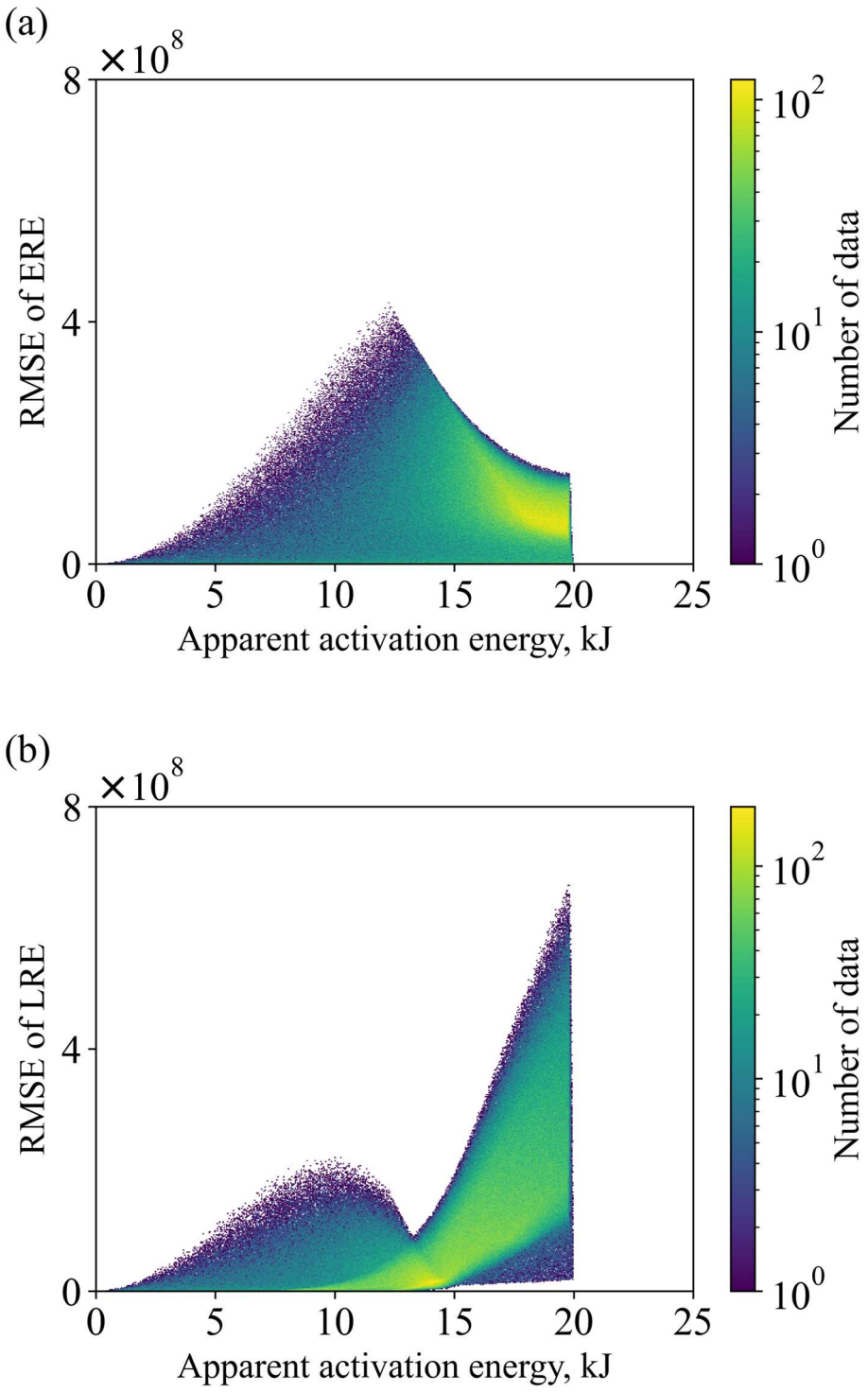


**Figure 2** Relationship between the apparent activation energy and the RMSE of the ERE (a) and LRE (b).

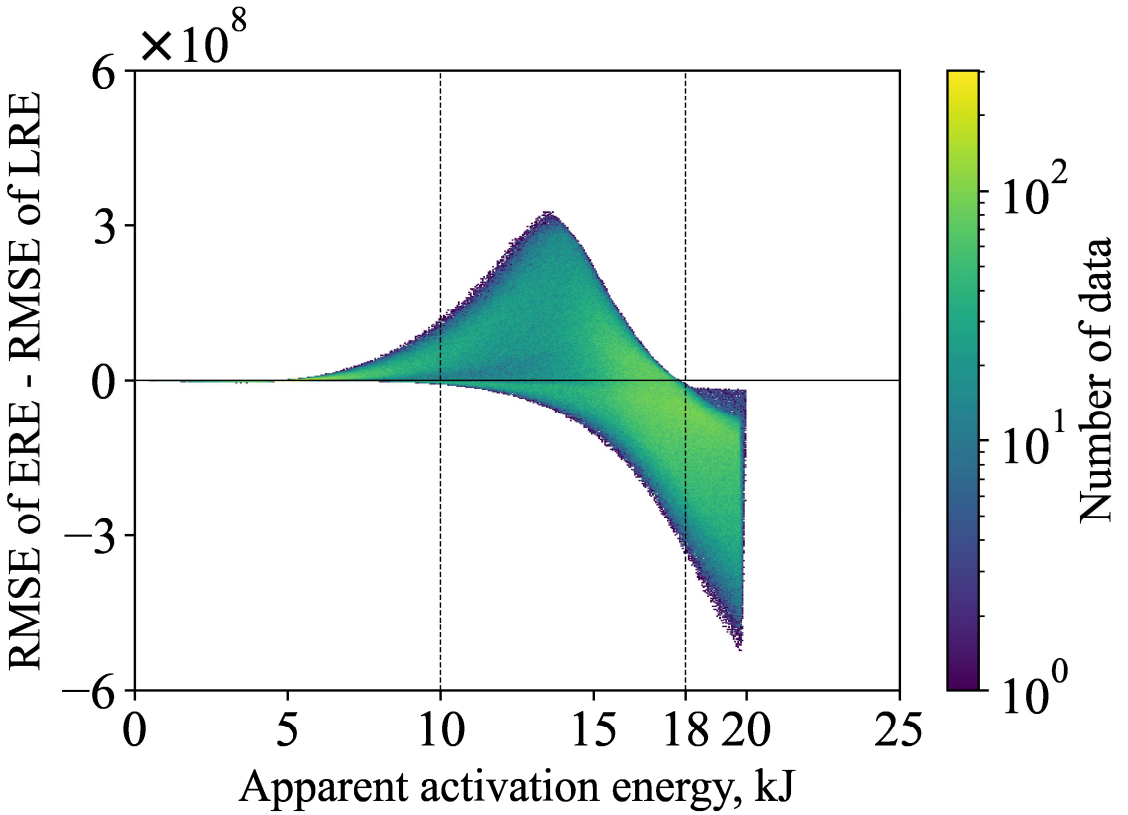


**Figure 3** Relationship between the apparent activation energy and the difference between the RMSE of the ERE and the LRE. A value above zero indicates that the LRE is better than the ERE, and a value below zero indicates that the ERE is better than the LRE.